HIGH POWER PROCESSING AT A HIGH ORDER MODE FREQUENCY

V. Volkov, BINP SB RAS, Novosibirsk, Russia,
J. Knobloch, A. Matveenko, A. Neumann, Helmholtz-Zentrum Berlin, Germany

Abstract

Regular High Power Processing (HPP) at fundamental frequency in a superconducting cavity usually carried out to increase maximal RF field in the cavity that is limited by Field Emission (FE). HPP at a High Order Mode (HOM) frequency allow significantly increasing FE threshold of fundamental RF field. In the paper we give proof of this prediction and give the concrete proposal of such HPP design for Rossendorf 3.5-cell RF gun structure. Expected RF over field is about 100% (from 17 up to 34 MV/m) as compared with a regular HPP.

INTRODUCTION

Dark current, or the unwanted field emission of electrons from nanoprotrusions (or asperities) localised on metal surfaces in the regions with high electric surface field is undesirable because it limits operational field and beam performance. Asperities are usually formed by dust particles that appear in a cavity during its assembly. There are difficulties to prove a perfect technology of such clean assembly if it takes place occasionally against those one that are made by manufacturers. The problem can be solved by the cavity treatment with considered HPP applied to melt the asperities. Such HPP is useful especially for SRF guns where a replaceable photo cathode inserted in it because there are real risks to import dust particles into SRF gun cavity through the insertion.

ASPERITY HEATING

Our estimations are based on a new conception of asperity heating that actualizes in rf and microwave cavities [1, 2]. It is heating due to rf skin current, not due to emission current or due to ion bombardment of the emitter surface as it seeks in present analysis (there is the comprehensive review in [3]). As some estimations and numerical simulation predicts [1] the rf skin current gives orders of magnitude large heating power in comparison to emission current heating power.

Rf skin current density is defined by Maxwell equation* [4]:

$$\boldsymbol{J} = rot(\boldsymbol{H}) - \partial \boldsymbol{D}/\partial t \qquad (1)$$

This current crosses through the asperity tip surface. Due to the enhancing rf field at the tip this current multiplied by enhancement factor β. This current propagates further along the asperity volume because the skin layer much large than the asperity diameter.

RF fields of TM mode in rf cavity could be expressed as $\boldsymbol{D}(\boldsymbol{r},t)=\boldsymbol{D}(\boldsymbol{r})\cdot e^{i\omega t}$ and $\boldsymbol{H}(\boldsymbol{r},t)=-i\omega\cdot\boldsymbol{H}(\boldsymbol{r})\cdot e^{i\omega t}/\omega_c$. Inserting it to Eq.(1) gives $\boldsymbol{J}=-i\omega\cdot e^{i\omega t}[rot(\boldsymbol{H})/\omega_c+\boldsymbol{D}]$, i.e. $J\sim\omega$.

Therefore the heating power is proportional to $P\sim\omega^2$ and the asperity temperature is proportional to $T\sim\omega^{1/2}$ which is determined by a balance of heating power and Boltzmann radiation. Here ω_c is a certain coefficient. The bold type symbols indicate vectors. The term of $rot(\boldsymbol{H})$ can be neglected near regions with high rf electric field in a cavity where the asperity dispositions are considered.

2D models of asperities [1, 2] shown in Fig.1 demonstrates electric field forces acting between the dust particle and the cavity surface. The same forces acts between two identical particles assuming the second particle is the mirror image in the cavity surface. These forces, between such electric dipoles, can be estimated (at $z>L$) by Coulomb law as $F\sim(q\cdot L)^2/z^4$, where the charge q can be calculated as the time integral of the current of Eq.1 propagating through the dipole asperity.

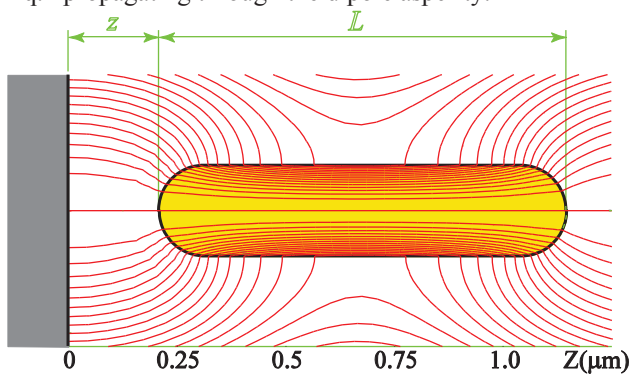

Figure 1: Numerically simulated RF field pattern of the asperity model ($L/r=10$) close a cavity wall.

Due to rf fields the asperities are directed along electric force lines due to the forces acting at the ends to the opposite sides. If the field has a gradient then the summary forces (F) not zeroing and acts to the direction with increased field. Magnetic force acts to the current perpendicularly to the asperity and to the magnetic field vector. In Fig.3 simulated with SLANS cod these forces are shown.

The main estimating formulas obtained in [1] are listed below - the electric force and temperature of asperities

$$F = 8\pi\varepsilon_o r^3\beta^2 E\frac{dE}{dL} \qquad (2)$$

$$T_{RF} = \beta\cdot[(\varepsilon_o E)^2\omega^2\rho r/4\sigma]^{1/4} \qquad (3)$$

Here are assumes $L/r=2\beta$, where r is the asperity radius, T_{RF} is emitter temperature, β is field enhancement factor, E is RF electric field, ω is RF circular frequency, ρ is electric conductivity, ε_o is electric constant, σ is Stephan-Boltzmann constant.

To corroborate the considered conceptions about the dust particle nature of FE in microwave cavities and the asperity heating we produce three experimental dates.

* Symbols adopted throughout this article unless otherwise noted are defined in the Handbook [4].

ISBN 978-3-95450-143-4

HZB Experiments

3D modelling of dark current trajectories emitting from the nanoprotrusion and hitting to the JYG screen in the RF gun cavity predicts the form of the screen image that was observed in HZB experiments [1] (see Fig.2). The cone angle of the image forms due to the diffusion of emitting electrons from the tip of the asperity having the specific rf field configuration with fan like distribution of field vectors. The asperity position must have some off-set relatively to the cavity axis. As the simulation predicts such an image cannot be done from a spot like emitter.

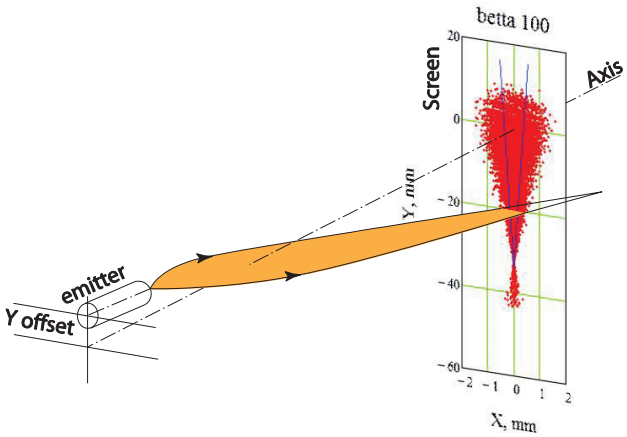

Figure 2: The scheme of numerical simulation of dark current trajectories emitted from the asperity disposed at the cavity back wall upon which they hit the YAG screen.

Light Emission Phenomena

The light emission phenomena in SRF cavity with flying point lights which observed with help of video camera [5] can be explained as the asperities heating by the skin current up to visible light temperature. The electric forces of Eq.2 compensate the asperity weight shown in Fig.3 in the region with positive F_E around the cavity axis and magnetic forces compensate centrifugal forces of asperity orbit. The asperities can have a positive charge due to FE therefore several particles must be orbited interactively as a one polygonal object.

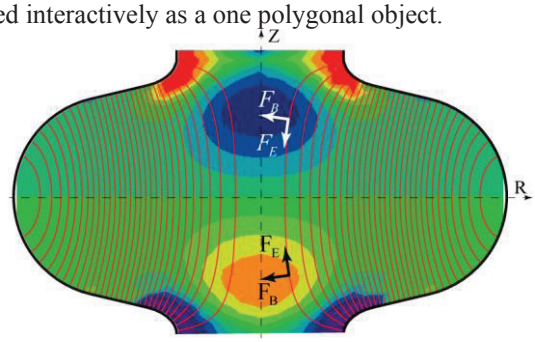

Figure 3: Electric (F_E) and magnetic (F_B~-R) forces acting on asperities in RF cavity. The "hot" colours indicate the regions with intensity of positive electric forces directed upward and "cold" colours indicates down directed electric forces.

Kilpatrick Criterion

The asperity heating (skin current) can be those physical causes of frequency dependent predictions made by the Kilpatrick criterion [4]. Existing FE theory based on Fouler-Nordheim equation does not give such an explanation [3].

If we consider T_{RF} in Eq.(3) is the maximal asperity temperature reached at HPP both in one of a cavity with ω resonance frequency and in other similar cavity having a higher resonance frequency (ω_{HF}) with the same configuration of RF electric field than the enhancement factor (β_{HF}) will be

$$\beta_{HF}=\beta\cdot(\omega/\omega_{HF})^{1/2}. \quad (4)$$

Therefore we can apply in the second cavity large electric field of main mode to get the same dark current. By using the equation $\beta_{HF}\cdot E_{HF}=\beta\cdot E$ that assumes equal dark currents we obtain equation similar to Kilpatrick criterion:

$$E_{HF}/E=\beta/\beta_{HF}=(\omega_{HF}/\omega)^{1/2} \quad (5)$$

HOM HPP

The experiments with dark current energy distributions in Rossendorf SRF gun [6] indicates the fact that main concentration of dark current sources are in the cathode cell, i.e. at the hole edge around the cathode. This conclusion becomes teachable due to numerical simulation of dark current trajectories of the experiments that is described in [2]. In this condition, the HOM of 2.842 GHz with maximal electric field in the cathode cell is the best candidate for HOM HPP. In Figure 4 the RF electric field pattern of this HOM and its amplitude distribution on axis are presented.

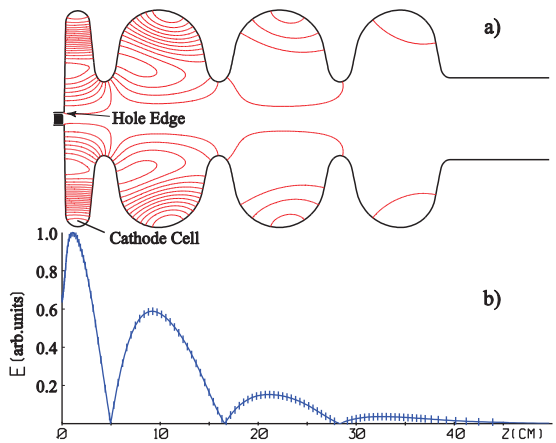

Figure 4: a) electric field pattern of HOM 2.842 GHz, b) HOM amplitude distribution of electric field on axis.

We compare the numerically simulated HOM HPP method applied for Rossendorf SRF gun with the regular HPP made in [6]. Gaussian temporal distribution of field emitted current with rms width of σ_{FE} is taking into account in the simulation.

$$\omega\cdot\sigma_{FE}=\left(\frac{\beta\cdot E}{2^{0.5}\cdot B_{FN}\cdot\phi^{1.5}}\right)^{0.5}, \quad (6)$$

where $B_{FN}=6.83\cdot10^6$, and $\phi=4.3$ eV is the work function.

Dark current trajectories from the hole edge around the cathode of the cavity with these considered HPP are simulated by ASTRA cod and depicted in Figs. 5a and 5b.

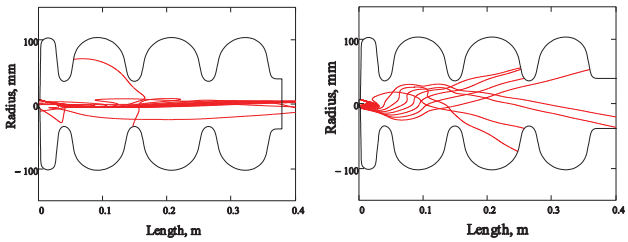

a) b)

Figure 5: Dark current trajectories in main mode field (a) and in HOM field (b).

In practice there is convenient to use a maximal power dissipated by dark currents with HOM HPP instead of the dark current magnitude because the limitation is due to the power limiting by HOM generator. In the example of Rossendorf SRF gun [6] the dark current power of main mode HPP was found to be 500 W by numerical simulation of dark current trajectories. We have simulated those HOM HPP lead to FE power up to 300 W with numerically simulated dark current trajectories caused by HOM field configuration. A pulse regime of operation goes without saying here.

If the field amplitude is raising in the cavity the asperity temperature comes up to a melting temperature and after that the decreasing of the enhancement factor β is beginning such that the temperature in Eq. 3 remains constant. We must take into account the difference between RF electric field configurations of two considered modes against the previous case of Eq.5 derivation, especially the difference of surface peak electric fields $E_o \neq E_{hom}$. Equating of two melting temperatures of Eq.3 for two considered HPP gives the relation

$$\beta_o / \beta_{hom} = (E_o \omega_o / E_{hom} \omega_{hom})^{1/2}, \qquad (7)$$

where E_o, E_{hom} are the peak electric fields and β_o, β_{hom} are the enhancement factors at the regular HPP [4] and HOM HPP correspondingly. We assume in Eq.3 the asperity radius (r) does not changed during the HPP and considered regular HPP enhancement factor is $\beta_o=575$.

We expect the field of main mode after the HOM HPP will be large by the factor of Eq.6 because such field gives the same dark current as one before the HPP. In Figure 6 calculated factors of Eq.6 named as Main mode gain and the dissipated FE power with HOM HPP are presented versus of HOM maximal field on axis.

We see in Fig.6, after the HOM processing we can raise the level of main mode field up to $E_{max}=16.7*2.1=35$ MV/m and we will have the same dark current from the hole edge where there is the main source of FE.

Main simulated parameters of two considered HPPs are presented in Table 1.

Table 1: Summary of Simulated Parameters

Parameter	1.3 GHz	2.842 GHz
Enhancement factor, β	575	270
Peak FE current, A	$4.3\cdot10^{-8}$	$2.47\cdot10^{-7}$
Rms width of FE bunch, ps	45	20.6
Maximal axis field, MV/m	16.7	23
Peak surface field, MV/m	20.24	42.4
FE dissipated power, W	500	300

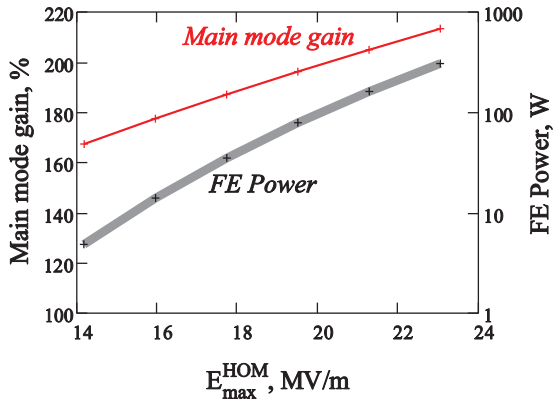

Figure 6: Field gain of main mode after the HOM HPP.

CONCLUSION

The new conception of asperity heating by RF skin current have met the confirmation by the HZB experiments, it may be the reason of the flying light emission phenomena, and it counts for the physical cause of frequency dependent predictions made by the Kilpatrick criterion.

Considered HOM HPP gain the accelerating field by factor of two in magnitude. This is especially useful for SRF guns due to a risk of a dust contamination of the cathode cell that may occur during the cathode insertion.

ACKNOWLEDGMENTS

The authors are thankful to HZDR team colleagues with head of J. Teichert for useful discussions.

REFERENCES

[1] V.Volkov et al., Interpretation of dark current experimental results in HZB SC RF gun, IPAC, 2012.
[2] V.Volkov, Numerical simulation of dark current and halo particles, Unwanted Beam Workshop, Berlin, 2012.
[3] K.L.Jensen et al., PRST-AB, **11**, 081001(2008).
[4] A.W.Chao, M.Tigner, Handbook of accelerators physics and engineering, 1998.
[5] P.L. Anthony et al., Experimental studies of light emission phenomena in superconducting RF cavities, NIM, A612, 1-45 (2009).
[6] R.Xiang et al., Dark current measurements at the ELBE SRF gun, Unwanted Beam Workshop, Berlin, 2012.

ISBN 978-3-95450-143-4